AFRL-OSR-VA-TR-2013-0498

SPIDER GLAND FLUIDS - FROM PROTEIN-RICH ISOTROPIC LIQUID TO INSOLUBLE SUPER FIBER

GREGORY HOLLAND

ARIZONA STATE UNIVERSITY

09/17/2013
Final Report

AIR FORCE RESEARCH LABORATORY
AF OFFICE OF SCIENTIFIC RESEARCH (AFOSR)/RSL
ARLINGTON, VIRGINIA 22203
AIR FORCE MATERIEL COMMAND

1. REPORT DATE **17 SEP 2013**	2. REPORT TYPE	3. DATES COVERED **15-06-2010 to 14-06-2013**

4. TITLE AND SUBTITLE **Spider Gland Fluids-From Protein-Rich Isotropic Liquid To Insoluble Super Fiber**	5a. CONTRACT NUMBER
	5b. GRANT NUMBER
	5c. PROGRAM ELEMENT NUMBER
6. AUTHOR(S)	5d. PROJECT NUMBER
	5e. TASK NUMBER
	5f. WORK UNIT NUMBER
7. PERFORMING ORGANIZATION NAME(S) AND ADDRESS(ES) **Arizona State University,Tempe,AZ,85281**	8. PERFORMING ORGANIZATION REPORT NUMBER
9. SPONSORING/MONITORING AGENCY NAME(S) AND ADDRESS(ES)	10. SPONSOR/MONITOR'S ACRONYM(S)
	11. SPONSOR/MONITOR'S REPORT NUMBER(S)

12. DISTRIBUTION/AVAILABILITY STATEMENT **Approved for public release; distribution unlimited**

13. SUPPLEMENTARY NOTES

14. ABSTRACT

15. SUBJECT TERMS

16. SECURITY CLASSIFICATION OF:			17. LIMITATION OF ABSTRACT	18. NUMBER OF PAGES	19a. NAME OF RESPONSIBLE PERSON
a. REPORT **unclassified**	b. ABSTRACT **unclassified**	c. THIS PAGE **unclassified**	**Same as Report (SAR)**	**29**	

1. Cover Sheet:

To: technicalreports@afosr.af.mil
Subject: Final Performance Report to Dr. Hugh DeLong

Contract/Grant Title: Spider Gland Fluids: From Protein-rich Isotropic Liquid to Insoluble Super Fiber

PIs: Gregory P. Holland and Jeffery L. Yarger

Institution: Department of Chemistry and Biochemistry, Arizona State University, Tempe AZ 85287-1604

Contract/Grant #: FA9550-10-1-0275

Reporting Period: 15 June 2010 to 14 June 2013

2. Objectives (taken directly from the original proposal):

Spider dragline silk is one of nature's highest performance fibers and has the potential for numerous military applications ranging from protective clothing to biological scaffolding and biomedical materials. However, for most applications we must first be able to produce the fiber in large quantities, and this requires that spider silk be produce biosynthetically in the laboratory. With the advent of DNA sequencing of numerous spider silks and the expression of these sequences in several different biological organisms, it was believed that this goal had been achieved. To date, however, numerous synthetic spider silks have been made with either partial or full primary amino acid sequence, but none match the mechanical strength of natural spider silk. This is primarily due to differences in fiber formation (engineering) and the resultant differences in secondary and tertiary structure of the silk proteins. Hence, the ability to reproduce spider silk fibers in the laboratory (synthetic silk), relies on a molecular understanding of how spiders produce insoluble silk fibers from an aqueous protein-rich isotropic liquid solution in the gland. The objective of the proposed research is to elucidate the interactions, mechanisms and chemistries of the spider silk producing process at the molecular level. Our primary focus is to characterize the protein-rich fluid in the major ampullate gland. We plan to utilize a combination of nuclear magnetic resonance (NMR) methods in conjunction with x-ray diffraction (XRD) in collaboration with Argonne National Laboratories (ANL) to achieve this goal. A list of specific aims that Profs. Holland and Yarger hope to achieve in the proposed research is given below:

- Conduct high-resolution magic angle spinning (HR-MAS) NMR spectroscopy of isotopically enriched major ampullate glands excised from different species of spider to characterize the structure of the spider silk proteins in the gland. This will involve completely assigning the ^1H, ^{13}C and ^{15}N NMR spectra of the proteins in the gland with multi-nuclear, multi-dimensional NMR methods to determine if the proteins in the gland exhibit secondary, tertiary and/or quaternary structure.
- Determine with HR-MAS NMR spectroscopy if changing the pH and/or temperature of the gland fluid promotes aggregation and/or protein folding into a β-sheet structure.
- Utilize modern solid-state NMR techniques (*e.g.* two-dimensional ^{13}C CP-MAS with dipolar recoupling) to characterize gland fluids that have been processed in various ways including dehydration, methanol treatment, solubilized in ionic liquids and exposed to mechanical stress. Establish the relevant processing conditions for converting the isotropic gland fluid to a fibrous material rich in crystalline β-sheets.
- Perform XRD measurements on gland fluids that have been processed under the above stated conditions to detect the presence of β-sheet or other crystalline structures. Utilize XRD methods to determine the domain size and dimensions of the crystalline component and compare to native spider silks.
- Develop magnetic resonance imaging (MRI) techniques to micro-image spider glands and ducts on in tact spiders and conduct localized NMR spectroscopy on the contents of the glands and ducts.

3.1 Status of Effort (Year 1):

The objective of this research is to elucidate the interactions, mechanisms and chemistries of the spider silk producing process at the molecular level. Our primary focus is to characterize the protein-rich fluid in the major ampullate gland. We have been using a suite of magnetic resonance (NMR and MRI) spectroscopic and X-ray diffraction (XRD) methods to uncover the fundamental molecular mechanisms for converting spider gland fluids to high performance fibers. We have established a method for isotopically (^{2}H/^{13}C/^{15}N) enriching the silk proteins within spider glands and conducted multi-dimensional, multi-nuclear high-resolution magic angle spinning (HR-MAS) NMR on excised spider glands. Our initial NMR measurements indicate that the silk proteins (MaSp1 and MaSp2) in the major ampullate gland are in a completely unstructured, random coil state prior to fiber formation. In addition, we have found that conditions for converting the isotopic gland fluid to an insoluble fibrous form rich in β-sheet structure depend on the ratio of the two proteins. Finally, we have succeeded in imaging the major ampullate gland with MRI on a live black widow spider and conducted localized spectroscopy on the gland contents.

3.2 Status of Effort (Year 2):

Our recently published ^{1}H and ^{13}C multi-dimensional HR-MAS NMR study illustrated that the spider silk proteins, major ampullate spidroin 1 and 2 (MaSp1 and MaSp2), are present in a completely unstructured, random coil state within the gland, prior to fiber formation (J.E. Jenkins et al. *Soft Matter* **2012**, *8*, 1947). This year we began investigating the backbone molecular dynamics of the unstructured silk proteins in the gland environment with conventional HR solution-state NMR techniques. Spin-lattice (T_1) and spin-spin (T_2) relaxation in conjunction with {^{1}H}^{15}N nuclear Overhauser enhancement (NOE) measurements indicate that the silk proteins are highly flexible exhibiting nanosecond timescale dynamics within the gland environment. The presence of these rapid local molecular dynamics permits the study of the native spider silk proteins with advanced three-dimensional (3D) liquid-state NMR regardless of the silk protein's large size (200 - 350 kDa). In addition, we have been using a combination of liquid-state and solid-state NMR to probe the impact of pH on the structure of the spider silk proteins and are beginning to establish the pH range that initiates native silk protein folding into fibrous β-sheet structures. In addition to NMR methods, we have been developing XRD methods in collaboration with ANL to probe β-sheet content, nanocrystallite size and morphology in natural spider silks and processed gland fluids. Lastly, we continue to develop MRI as an *in situ* tool for interrogating silk protein structure and dynamics within the various silk glands.

3.2 Status of Effort (Year 3):

In the final year of the award, we continued to develop solution- and solid-state NMR methods to characterize the structure and dynamics of spider silk proteins. Our research team developed ^{1}H solution-state NMR methods to track isotope enrichment in spider silks. It is important for advanced solid-state NMR methods that we are able to determine precisely (site-specifically) where the isotopes are incorporated. Additionally, we were able to show that ^{1}H solution-state NMR can be used for amino acid analysis (AAA) of hydrolyzed silks without chromatographic separation. Although this NMR approach requires considerably more sample compared to conventional, chromatography based AAA, NMR is much more precise. This work was able to show that Pro contents

can be quite heterogeneous across silk samples while, the other amino acids were not. We continued developing solid-state NMR techniques to characterize backbone and side-chain dynamics with a newly designed ^{2}H-^{13}C 2D heteronuclear correlation (HETCOR) approach. We used this method to characterize molecular dynamics in spider silk fibers that provide considerable insight into chain packing and silk self-assembly. Finally, we continued to develop MRI methods for probing silk production *in situ* and Brillouin spectroscopy as a non-invasive tool to characterize silk mechanical properties.

Fig. 1 Picture of an excised *N. clavipes* major ampullate gland with tail, duct, and spinneret. The major ampullate spidroin 1 (MaSp1) and 2 (MaSp2) proteins are produced in the tail and then stored in the gland. The proteins travel through the duct and out the spinneret to form the dragline silk fiber.

4.1 Accomplishments/New Findings (Year 1):

Dragline spider silk is composed of two proteins, major ampullate spidroin 1 and 2 (MaSp1/MaSp2) that are produced in the major ampullate (MA) gland within the spider's abdomen. A photograph of a dissected *N. clavipes* MA gland is presented in Fig. 1 and details the process of MaSp1 and 2 production and formation into a silk fiber. Both proteins are synthesized in the tail of the MA gland and then stored as a concentrated aqueous solution that is ~50% protein w/v. For silk formation, the proteins flow from the gland down a long duct that narrows into the spinneret organ. The silk is pulled from the spinneret as the final water insoluble silk fiber. The process that the two proteins in an aqueous environment undergo to produce 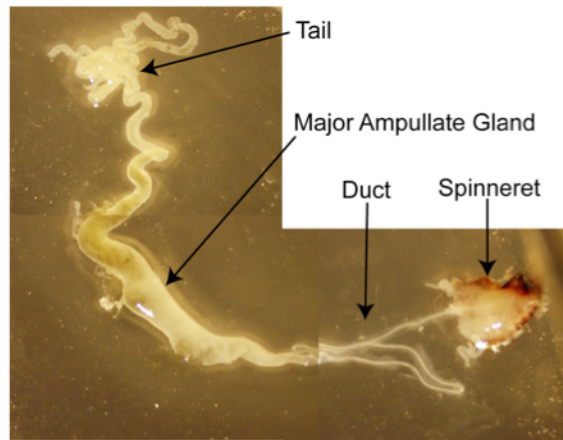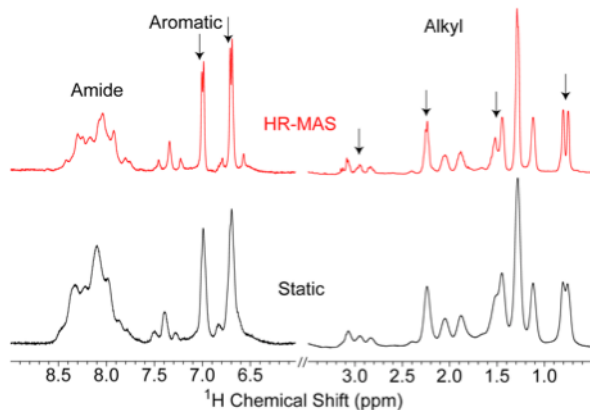nature's "super" fiber remains unclear. There is some evidence that dehydration and pH variation within the duct could play a role in converting the aqueous spinning dope to an insoluble fiber rich in β-sheet structure. A more thorough understanding of how the proteins behave in the gland, as well as out of the gland should assist in understanding the silk producing process and guide the engineering of usable synthetic fibers based on spider silk proteins. A fundamental understanding of the spider silk protein structure and chemistry in the gland environment should provide basic information that will assist in understanding the underlying problems

Fig. 2 Proton (^{1}H) NMR spectrum of freshly excised *N. clavipes* major ampullate glands. Spectra were collected static (black) and with HR-MAS at 10 kHz MAS (red). Arrows indicate enhanced resolution when HR-MAS is applied. Both spectra were collected with optimal shimming conditions.

with synthetic silk formation and production. We believe that a better understanding of this process will help advance synthetic silk-based materials for Air Force applications.

We have been studying the secondary structure (protein folding) of the spider silk proteins within the gland fluid with a method called High-Resolution Magic Angle Spinning (HR-MAS) NMR spectroscopy. HR-MAS is a magnetic resonance technique that is at the interface between liquid-state and solid-state NMR. It combines MAS to average residual dipolar interactions and bulk magnetic susceptibility broadening with a lock channel and a magic angle gradient that allows for liquid-state NMR techniques such as gradient coherence selection, water suppression, and pulsed field gradient self-diffusion measurements. HR-MAS NMR has been shown to be a powerful tool for studying soft matter materials and is particularly well suited for the study of excised tissues. We have found that HR-MAS NMR is an ideal magnetic resonance method for studying the spider silk proteins within intact excised MA glands. Comparisons are being made between the protein structures in the aqueous gland environment for two species of orb weaving spiders, *Nephila clavipes* and *Argiope aurantia*. The *Nephila clavipes* spider spins MaSp1-rich dragline silk (~80:20, MaSp1:MaSp2) while, *Argiope aurantia* spins MaSp2-rich spider dragline silk (~40:60, MaSp1:MaSp2). Thus, by studying these two different species we can focus on the structure of the two different proteins that make up spider dragline silk.

The fluid within the MA gland is a viscous protein solution (~50% protein w/v) that exhibits enhanced resolution
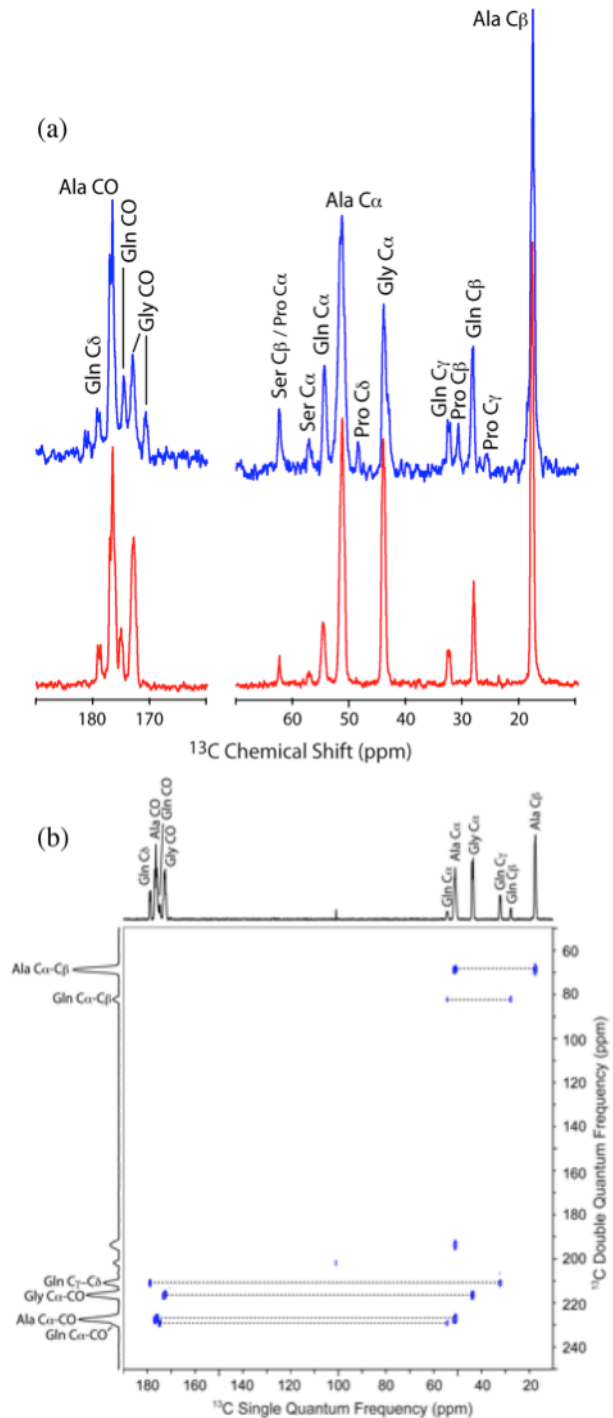

Fig. 3 The (a) ^{13}C direct HR-MAS NMR spectra of freshly excised ^{13}C/^{15}N-alanine enriched *A. aurantia* (blue) and *N. clavipes* (red) major ampullate glands. The (b) HR-MAS through-bond DQ/SQ ^{13}C correlation NMR spectrum collected with the INADEQUATE pulse sequence for the *N. clavipes* major ampullate glands. The INADEQUATE spectrum provides the ^{13}C chemical shift assignments for the ^{13}C direct spectra.

in the ^{1}H NMR spectrum when MAS is applied (see Fig. 2). Resolution enhancement is observed for the ^{1}H spectrum of *Nephila clavipes* MA gland in all regions of the spectrum when under 10 kHz MAS compared to the static (no MAS) ^{1}H spectrum. Typical linewidths for the ^{1}H HR-MAS spectrum are ~10–20 Hz depending on the amino acid environment. Of particular interest is the observation of the proton *J*-couplings (~6–10 Hz) for a number of amino acid sites in the ^{1}H HR-MAS spectrum. These *J*-splittings are absent in the static spectrum. An ability to resolve the *J*-couplings is useful when assigning the NMR spectra for these systems because they provide information regarding nearest neighbor bonding.

In order to better probe the structure of spider silk proteins within the MA gland, the proteins were isotopically (^{13}C/^{15}N) enriched prior to gland dissection to enable multi-dimensional, multinuclear HR-MAS NMR experiments. The ^{13}C HR-MAS NMR spectrum of MA glands excised from *Nephila clavipes* and *Argiope aurantia* spiders that were fed ^{13}C/^{15}N-Ala are displayed in Fig. 3a. The ^{13}C resonances display linewidths that are ~50-100 Hz. The broader line widths observed here can be attributed to the ^{13}C isotopic enrichment and resulting [13]C-[13]C *J*-coupling contributing to the linewidth. The presence of strong [13]C-[13]C *J*-coupling is further confirmed by observation of the [13]C-[13]C *J*-splitting (~50 Hz) for the Ala Cα and CO resonances. However, ^{13}C-enrichment is not observed exclusively for Ala, but rather ^{13}C-enrichment is obtained for Gly, Ala, Gln and Ser. These four amino acids constitute 73% and 85% of *Argiope aurantia* and *Nephila clavipes* spider dragline silk. Thus, a considerable fraction of the spider silk proteins in the MA gland can be isotope labeled by feeding solely ^{13}C/^{15}N-Ala. In addition to the Gly, Ala, Gln and Ser resonances, there appears to be evidence for weak Pro resonances for the *Argiope aurantia* MA gland (see Fig. 3a). The Pro resonance assignment is confirmed by isopically labeleing the *Argiope aurantia* MA gland with ^{13}C/^{15}N-Pro (see below).

Although we have not yet quantitatively assessed the ^{13}C enrichment, it is high enough to enable through-bond two-dimensional (2D) double quantum/single quantum (DQ/SQ) Incredible Natural Abundance DoublE QUAntum Transfer Experiment (INADEQUATE) spectra (see Fig. 3b) to be collected in a
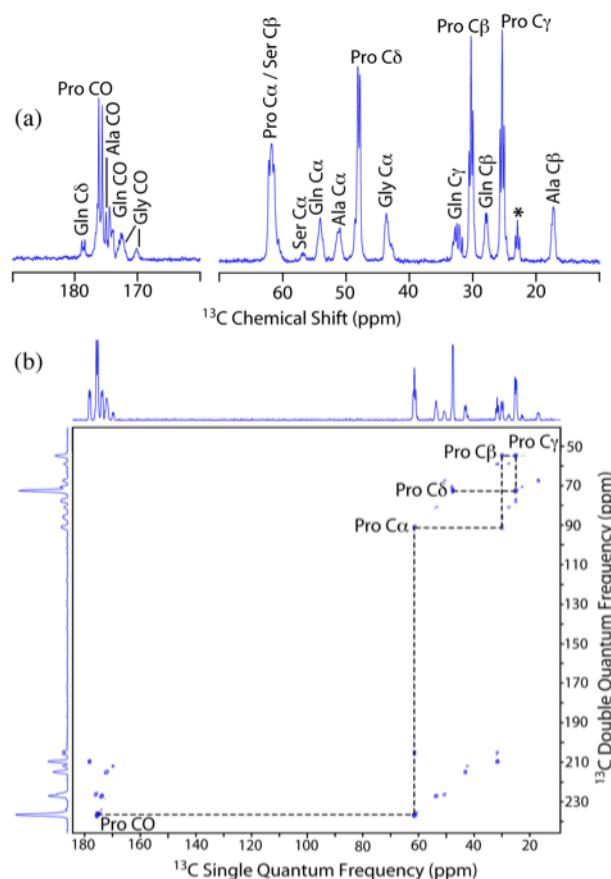

Fig. 4 The (a) ^{13}C HR-MAS NMR spectra of ^{13}C/^{15}N-proline enriched *A. aurantia* MA glands. The (b) HR-MAS DQ/SQ ^{13}C correlation NMR spectrum collected with the INADEQUATE pulse sequence. The INADEQUATE spectrum provides the ^{13}C chemical shift assignments for Pro. The [13]C-^{13}C spin connectivity is traced out for Pro.

reasonable time frame (1 - 2 days). This experiment provides an unambiguous ^{13}C assignment for the labeled amino acid sites (Gly, Ala, Gln, Ser) including the carbonyl resonances. All the unambiguously assignable ^{13}C isotropic chemical shifts are listed in Tab. 1. The assignment and chemical shifts extracted from the 2D DQ/SQ INADEQUATE

Table 1 **Carbon-13 isotropic chemical shifts (ppm) of spider silk proteins in the MA gland from HR-MAS NMR, random coil conformation, and average β-sheet and α-helical conformations (all chemical shifts are referenced to TMS)**

	A. aurantia Gland	*N clavipes* Gland	Random Coil	β-sheet	α-helix
Ala C_α	**50.9**	**51.1**	**50.8**	49.4	53.4
Ala C_β	**17.4**	**17.5**	**17.4**	20.3	15.4
Ala CO	**176.3**	**176.3**	**176.1**	174.7	177.8
Gly C_α	**43.0, 43.8**	**43.8**	**43.4**	42.0	46.0
Gly CO	**170.1, 172.5**	**172.6**	**173.2**	171.8	174.9
Gln C_α	**54.3**	**54.8**	**54.0**	52.6	56.6
Gln C_β	**28.1**	**27.8**	**27.7**	29.5	26.0
Gln C_γ	**32.3**	**32.2**	**32.0**	-	-
Gln C_δ	**178.9**	**178.7**	**178.8**	-	-
Gln CO	**174.2**	**174.8**	**174.3**	172.9	176.0
Pro C_α	**61.9**	**-**	**61.6**	60.2	64.2
Pro C_β	**30.4**	**-**	**30.4**		
Pro C_γ	**25.5**	**-**	**25.5**	-	-
Pro C_δ	**48.1**	**-**	**48.1**	-	-
Pro CO	**176.0**	**-**	**175.6**	174.2	177.3
Ser C_α	**57.0**	**56.9**	**56.6**	55.2	59.2
Ser C_β	**62.3**	**62.2**	**62.1**	63.1	60.7
SerCO	**173.0**	**-**	**172.9**	171.5	174.6

experiment was nearly identical for the two species of spider (see Tab. 1). These results provide the first NMR assignment for MA glands from the *Argiope aurantia* spider that produces a dragline silk with a high Pro content and thus, high in MaSp2.To confirm that the weak Pro resonances observed in the ^{13}C HR-MAS NMR spectrum of *Argiope aurantia* MA glands were indeed originating from Pro (Fig. 3a), a set of spiders were fed an aqueous solution of U-[^{13}C/^{15}N]-Pro to isotopically label proline and characterize its structure. The ^{13}C HR-MAS spectrum of ^{13}C/^{15}N-Pro labeled *Argiope aurantia* MA glands is displayed in Fig. 4. As expected, the weak resonances assigned to Pro in the ^{13}C/^{15}N-Ala labeled *Argiope aurantia* sample (Fig. 3a) greatly increase in intensity in comparison to the Gly, Ala, and Ser resonances and display resolvable [13]C-[13]C *J*-splittings for the Pro sites. This indicates a high level of isotope incorporation and enables a 2D ^{13}C DQ/SQ INADEQUATE experiment to be performed to obtain the resonance assignment for Pro (see Fig. 4b for Pro spin connectivity). An ability to obtain a complete NMR assignment for Gly, Ala, Gln, and Ser for two different species of orb weavers allows an assessment of the folded structure of the proteins within the intact MA gland to be made. In addition, the assignment of Pro in *Argiope aurantia* MA gland proteins allows for sole structural characterization of MaSp2 because essentially no Pro is found in MaSp1. The MA silk gland protein ^{13}C chemical shifts are tabulated in Tab. 1 along with the known ^{13}C chemical shifts for random coil, β-sheet, and α-helical secondary structures. Comparing the ^{13}C chemical shift for each resonance with known chemical shifts of amino acids adopting known protein secondary structure indicates that the proteins in the gland adopt a random coil structure. Thus, neither protein MaSp1 nor MaSp2 exhibits any secondary structure in the gland environment. It is interesting to note that not only are the β-sheet structures absent for the silk proteins in the MA glands but, β-turn and 3_1-helical structures present in the final silk fiber appear to be absent as well illustrating that these structures are only present in the final solidified dragline silk.

In order to further characterize the protein structure in the MA gland, ^{13}C/^{1}H HSQC

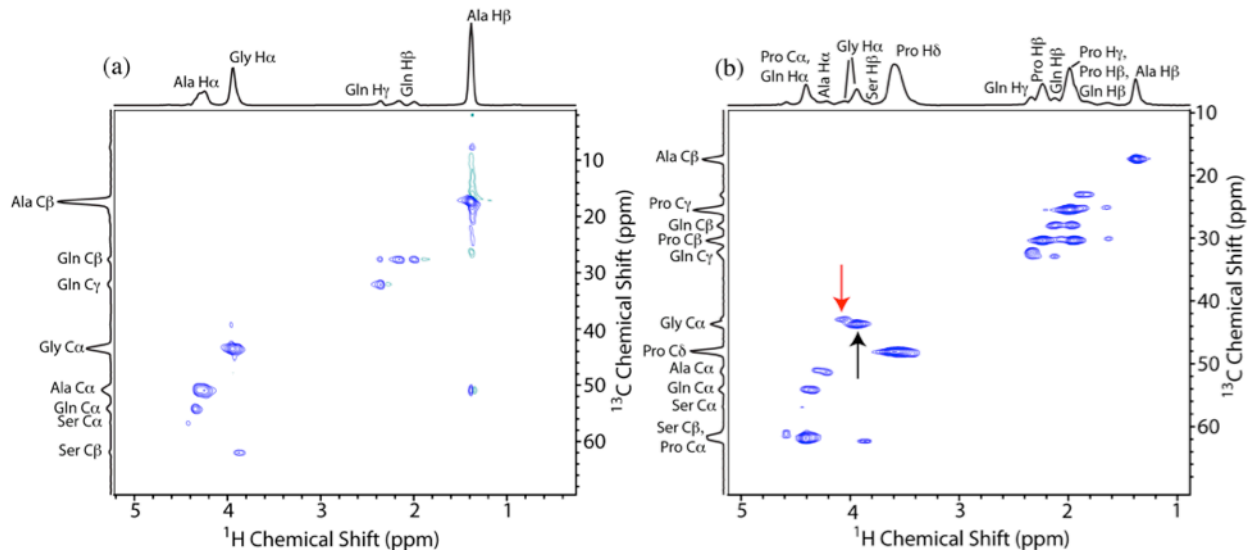**Figure 5.** The ^{13}C/^{1}H HSQC HR-MAS NMR spectra of freshly excised (a) ^{13}C/^{15}N-alanine enriched *Nephila clavipes* and (b) ^{13}C/^{15}N-proline enriched *Argiope aurantia* major ampullate glands (the arrows indicate two distinct Gly sites).

HR-MAS NMR spectra were collected to obtain the ^{1}H isotropic chemical shifts (see Fig. 5). Here we can utilize the ^{13}C chemical shift assignment obtained from the ^{13}C DQ/SQ INADEQUATE experiments (Fig. 3 and Fig. 4) to assign the ^{1}H dimension. The extracted ^{1}H chemicals shifts are listed in Tab. 2 along with the Hα chemical shifts that are dependent on backbone conformation. In agreement with ^{13}C chemical shifts (see Tab. 1), the Hα chemical shift indicate a random coil conformation for the proteins contained within MA glands from both species of spider (see Tab. 2).

The ^{1}H and ^{13}C chemical shift results from HR-MAS NMR spectroscopy has allowed us to investigate the folded structure of the spider silk proteins, MaSp1 and MaSp2, within excised MA glands. Prior to fiber formation, there appears to be no evidence that protein folding occurs within the MA gland of either the *Argiope aurantia* or *Nephila clavipes* spider and the proteins within the gland are simply in a pre-folded, random coil state. By utilizing the *Argiope aurantia* species that has a higher Pro content, the MaSp2 protein could be targeted and illustrate that in addition to MaSp1, it too exhibits a random coil structure within the MA gland. We are currently in the process of confirming these results by conducting relaxation measurements to determine whether the proteins are present in a true unfolded random coil state or a partially folded molten globule state. In addition, we continue to use HR-MAS NMR spectroscopy to study the mechanisms and chemistries that occur to convert the unstructured isotropic gland fluid to a spider silk fiber rich in secondary structure. Understanding the role of pH and ionic strength in fiber formation are currently underway in our laboratory.

Table 2 Proton chemical shifts (ppm) of spider silk proteins in the MA gland from HR-MAS NMR, random coil conformation, and average β-sheet and α-helical conformation (all chemical shifts are referenced to TMS)

	A. aurantia Gland	*N. clavipes* Gland	Random Coil	β-sheet	α-helix
Ala H_α	**4.26**	**4.27**	**4.32**	4.70	3.94
Ala H_β	1.38	1.38	1.39	-	-
Gly H_α	**3.94, 4.06**	**3.93**	**3.96**	4.34	3.58
Gln H_α	**4.36**	**4.34**	**4.34**	4.72	3.96
Gln H_β	1.97, 2.12	1.98, 2.14	1.99, 2.12	-	-
Gln H_γ	2.34	2.35	2.36	-	-
Pro H_α	**4.41**	**-**	**4.42**	4.80	4.04
Pro H_β	1.95, 2.24	-	1.94, 2.29	-	-
Pro H_γ	1.99	-	2.02	-	-
Pro H_δ	3.59	-	3.63	-	-
Ser H_α	**4.44**	**4.42**	**4.47**	4.85	4.09
Ser H_β	3.86	3.86	3.87, 3.89	-	-

In addition to applying HR-MAS NMR to probe the spider silk protein structure within the MA gland environment, we have been exploring the effect of dehydration and mechanical shear on the gland fluid by studying processed glands with ^{13}C cross-polarization (CP)-MAS solid-state NMR. We have looked at the effect of dehydration and shearing on the glands extracted from both *Nephila clavipes* and *Argiope aurantia* spiders (see Fig. 6). The interesting result here is a
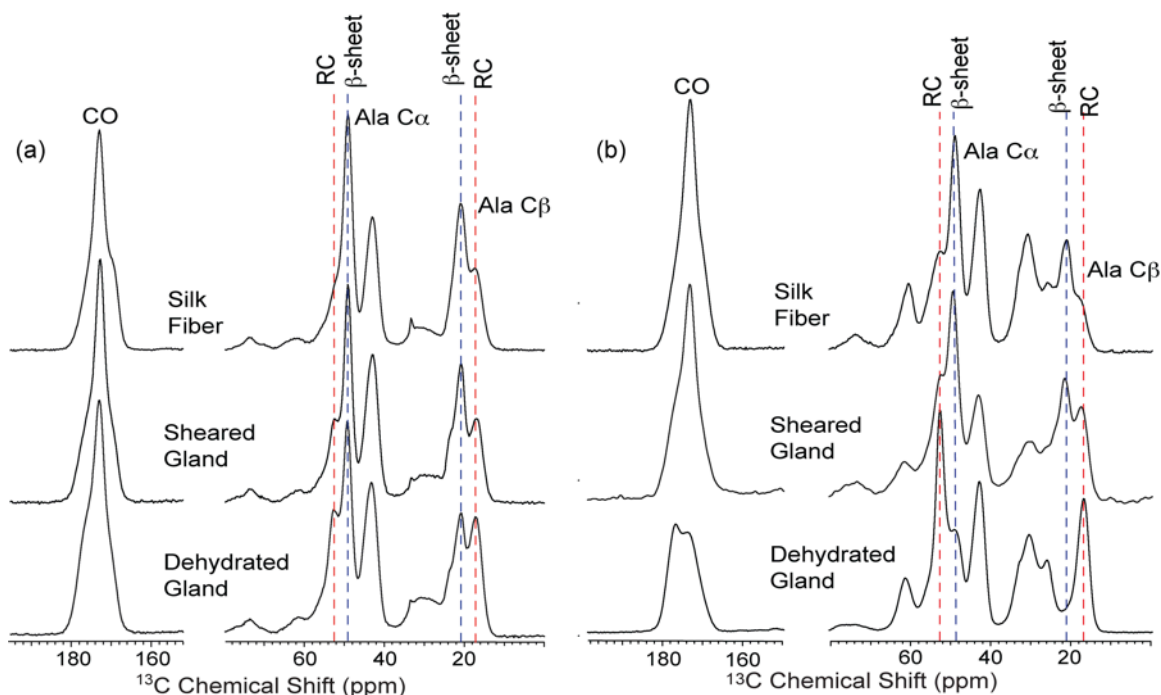
Figure 6. The solid-state ^{13}C CP-MAS NMR spectrum of dehydrated and mechanically sheared glands for (a) $^{13}C/^{15}N$-alanine enriched *Nephila clavipes* and (b) $^{13}C/^{15}N$-alanine enriched *Argiope aurantia*. The final dragline silk fiber collected from the same spiders is shown for comparison purposes. The Ala resonances associated with random coil (RC) and β-sheet structures are indicated in the figure.

dramatic difference between the two gland fluids for converting to a β-sheet structure upon dehydration. For the *Nephila clavipes* species, ~50% of the poly(Ala) is converted to a β-sheet structure just by dehydrating the gland at ambient laboratory conditions while the *Argiope aurantia* gland showed essentially no conversion to β-sheet under the same conditions. We have conducted this experiment three times to assure that this is real effect and got the same result each time. Mechanical shearing appears to increase the conversion to a β-sheet for both species however, neither processing conditions yield a gland spectrum that truly matches the ^{13}C CP-MAS spectrum observed for the silk fiber.

The stark contrast between the behavior of the two glands upon dehydration is believed to result from the different proline contents and thus, MaSp2 contents for the two species. The *Nephila clavipes* has a considerably higher MaSp1 content (~80%) and the *Argiope aurantia* has a higher MaSp2 content (~60%). These results seem to indicate that MaSp1 is a β-sheet templating agent while, gland fluids rich in MaSp2 (and proline) do not readily convert to a β-sheet without the addition of physical processing (i.e. mechanical shear stress). Understanding how the ratio of the two proteins influences the processing conditions is important for the production of synthetic spider silks. We have transferred this knowledge to Randy Lewis' group at Utah St. University (also in the AFOSR Natural Materials Program) who is producing recombinant spider silk proteins and spinning synthetic fibers. The Lewis group has produced two sets of synthetic dragline silk fibers that have MaSp1:MaSp2 ratios that mimic the *Nephila clavipes* and *Argiope aurantia* species. Our group has conducted ^{13}C CP-MAS NMR on this set of synthetic fibers and the results are depicted in Fig. 7. There is a distinct difference between the two sets of synthetic spider silks that matches the results from the natural
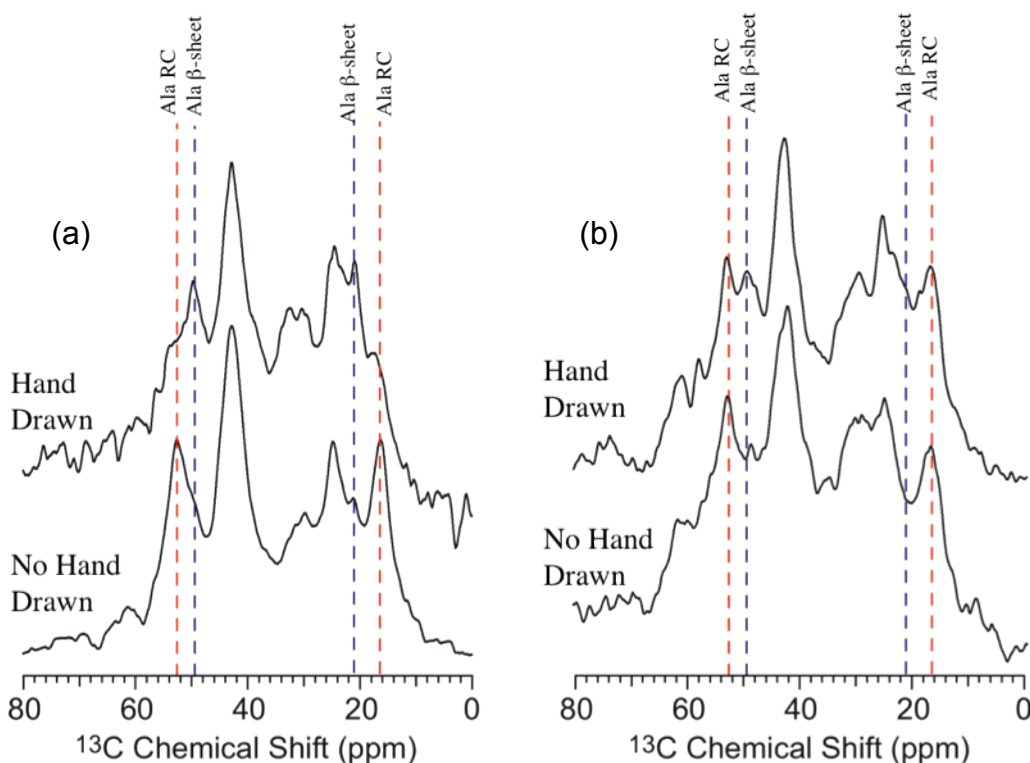
Fig. 7 The solid-state ^{13}C CP-MAS NMR spectrum of synthetic spider silk fibers derived from recombinant MaSp1 and MaSp2 proteins. The synthetic silk fibers have an MaSp1:MaSp2 ratio of (a) 80:20 (mimics *Nephila clavipes* dragline) and (b) 50:50 (mimics *Argiope aurantia* dragline). The Ala resonances associated with random coil (RC) and β-sheet structures are indicated in the figure.

gland material presented in Fig. 6. Specifically, the synthetic silk fiber with a MaSp1:MaSp2 ratio that matches *Nephila clavipes* (80:20) clearly displays a higher β-sheet content for poly(Ala) compared to the synthetic fiber that has a MaSp1:MaSp2 ratio that closely matches *Argiope aurantia* (50:50). In addition, a hand drawing process greatly increases the β-sheet fraction similarly to the mechanical shear processing on the natural fibers (see Fig. 6). These results on synthetic spider silk fibers illustrate that the information from processing and structural characterization of natural gland fluids with solid-state NMR can be used to guide the production of synthetic spider silk fibers that more closely match native spider silk. It should be noted that the β-sheet content in the synthetic spider silks is not quite as high as that observed in natural spider silk indicating that the processing conditions can still be optimized further. We feel that the studies on processing and structural characterization of natural spider silk dope from the gland will accelerate the advancement of spider silk-based materials for Air Force applications.

In addition to applying *ex situ* techniques to structurally characterize spider silk and the silk producing process, we have been developing magnetic resonance imaging (MRI) methods to characterize spider silk production *in situ* on live spiders. MRI images of the silk producing glands within the abdomen of a live Black Widow (*Latrodectus hesperus*) spider are shown in Fig. 8. These images were collected on an 800 MHz NMR spectrometer equipped with a specially designed micro-imaging probe. The images are of excellent quality and the silk protein producing glands and ducts can be readily

observed in the images. For example, in the top down view (slicing from the spiders back down) the pair of major ampullate glands is observed as two circles (Fig. 7a, indicated in red). The profile view (Fig. 7b) clearly shows the known tear-drop shape of the MA gland along with the connected ducts that lead to the spinneret. This tear-drop shaped image of the MA gland is very similar to what is observed when the gland is carefully dissected from the spider's abdomen (see Fig. 1). However, in contrast with the HR-MAS methods discussed above for studying excised glands, the MRI method allows us to characterize the gland in a nondestructive manner, on a live spider, *in situ* without perturbing the spider in any way.

We are working towards coupling MRI with localized magnetic resonance spectroscopy (MRS) on live spiders. This approach will
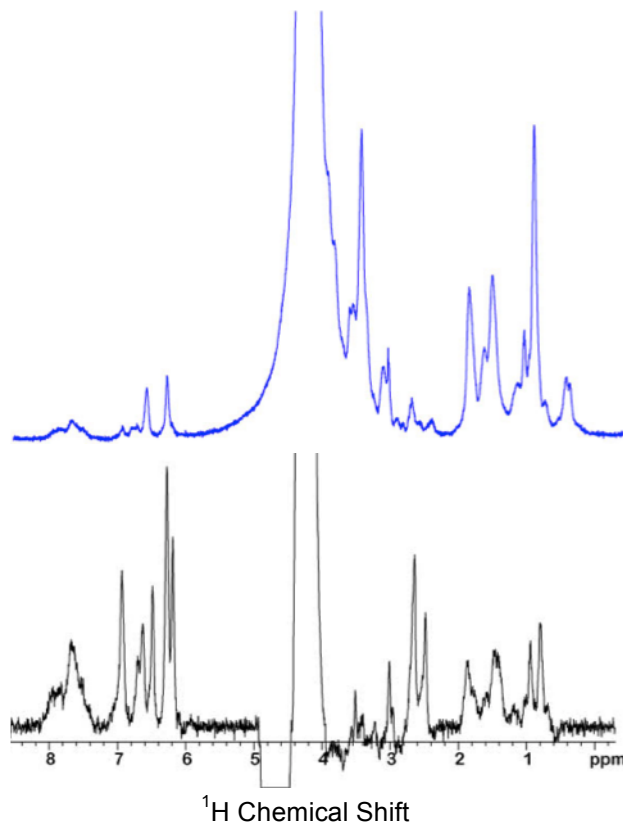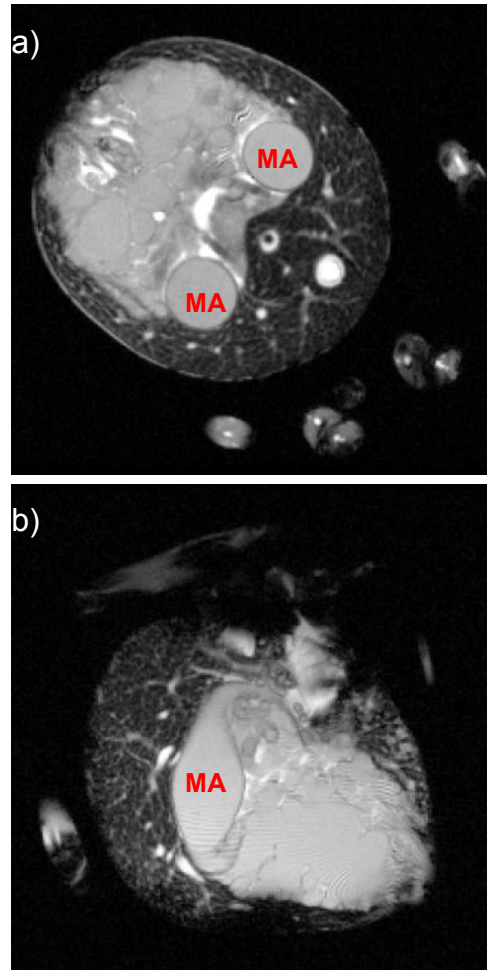

Fig. 8 MRI images of the silk producing glands and ducts within the abdomen of a live Black Widow spider. The (a) top down view and (b) profile view of the glands is shown. The two major ampullate glands (MA) are indicated in red.

¹H Chemical Shift

Fig. 9 Comparison of (a) ^{1}H HR-MAS NMR spectrum of excised (*ex situ*) *A. aurantia* major ampullate glands and (b) ^{1}H MRS spectrum with micro-imaging on 150 μm^3 volume (*in situ*) of the major ampullate gland for a living *A. aurantia* spider.

allows us to do ^{1}H NMR spectroscopy on the gland and duct contents in combination with micro-imaging. An ability to conduct NMR spectroscopy in combination with MRI will provide us with a structural probe to track protein folding, structural changes and pH variation that occurs in the gland and ducts. An example of our first ^{1}H MRS spectrum collected on a 150 μm^3 volume within the major ampullate gland of an *Argiope aurantia* spider is shown in Fig. 9. This spectrum is compared to the ^{1}H HR-MAS spectrum

collected from an excised *Argiope aurantia* MA gland. There are some distinct similarities between the two spectra and there are some substantial differences. We are currently in the process of assigning the MRS spectrum and discerning the cause for the differences. Development of this technique is an ongoing project in the laboratory that involves writing new pulse sequences to improve data collection of images and localized MRS spectra. We feel that an *in situ* technique to study the spider silk process has been lacking and should help better elucidate the conversion process at the molecular level from isotropic liquid in the gland to insoluble fiber with outstanding mechanical properties. It is our hope that the development of this tool in conjunction with the previously described methods will provide the information necessary to produce spider silk based materials for Air Force applications.

4.2 Accomplishments/New Findings (Year 2):

Our recently published HR-MAS NMR work on MaSp1 and MaSp2 spider silk proteins within the major ampullate glands of *Argiope aurantia* and *Nephila clavipes* spiders indicated that both silk proteins are completely unstructured in the gland (J.E. Jenkins et al. *Soft Matter* **2012**, *8*, 1947). This interpretation is based solely on the conformation dependence of the ^{13}C and ^{1}H isotropic chemical shifts extracted from the NMR spectra. In order to confirm this study, we have been exploring the structure of the MaSp1 and MaSp2 silk proteins produced by the *Black widow* species. Similar results were obtained compared to the *Argiope aurantia* and *Nephila clavipes* spider, the NMR secondary chemical shift analysis indicate the proteins are random coil prior to fiber formation (data not shown). We have continued to explore the *Black widow* (*Latrodectus hesperus*) species because they are readily available to us in the southwest and more importantly, the complete MaSp1 and MaSp2 primary sequence is known for this species (N.A. Ayoub et al. *PLoS ONE* **2007**, e514).

Fig. 10 The ^{1}H liquid-state NMR spectrum of major ampullate glands excised from *Black widow* spiders. The spectrum was collected in (black) 90:10 $H_2O:D_2O$ and (blue) 99.9% D_2O. The spectrum of the glands with 99.9% D_2O solvent was collected 5 minutes after the sample was prepared. Almost complete exchange of the NH protons is observed in 5 mins.

We have now illustrated that the major ampullate silk proteins from three species of spider appear to have a random coil structure from NMR isotropic chemical shift analysis. However, it should be noted that the proteins could indeed be partially folded and undergo rapid conformational exchange on the chemical shift timescale (μs-ms) yielding random coil shifts even for a partially folded molten globule or intrinsically disordered protein (see Ohgushi et al. *FEBS Lett*. **1983**, *164*, 21). In order to corroborate the results from NMR chemical shift analysis, we have begun a series of experiments where the exchange rates of the amide protons (NH) are probed. An example is shown in Fig. 10, where the exchange of the amide protons is monitored by exposing the major
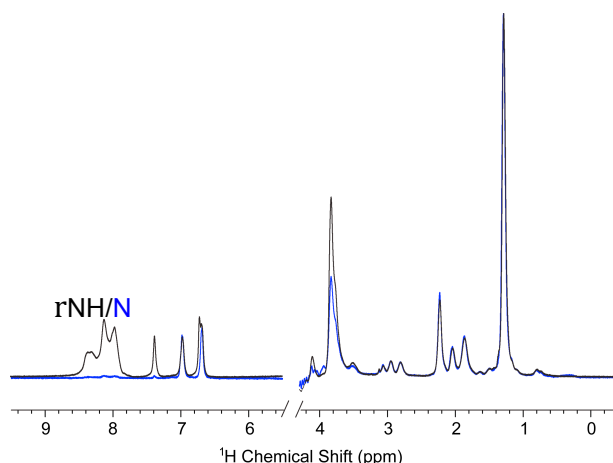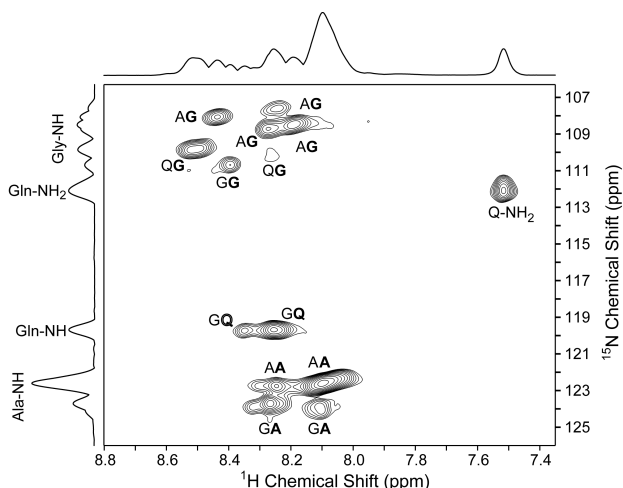
Fig. 11 ^{15}N/^{1}H HSQC liquid-state NMR spectrum of ^{15}N-alanine labeled major ampullate gland excised from the *Black widow* spider. The resonance assignment is shown in single letter amino acid code. The sequential assignment is based on 3D liquid-state NMR experiments discussed below.

ampullate gland containing the silk proteins to 99.9% D_2O and monitor the NH proton resonances as a function of time. Interestingly, 95% of the NH resonances completely exchange within 5 minutes of exposing the sample to D_2O. For folded proteins that exhibit defined secondary and tertiary structure, the NH protons are strongly hydrogen-bonded and exhibit exchange rates on the order of hours to days. This result confirms the chemical shift analysis and supports a completely unfolded, random coil state for the spider silk proteins within the major ampullate gland.

Recently, we began exploring the utility of conventional high-resolution (HR) solution-state NMR spectroscopy for probing the structure and dynamics of spider silk proteins within the major ampullate gland of *Black widow* spiders. A ^{15}N/^{1}H heteronuclear single quantum correlation (HSQC) spectrum for ^{15}N-alanine enriched major ampullate glands excised from *Black widow* spiders collected with a conventional solution-state NMR probe is shown in Fig. 11. Surprisingly, a well-resolved ^{15}N/^{1}H HSQC spectrum is observed with 13 unique backbone resonances resolved. The reason this result is surprising is due to the fact that the predicted overall rotational correlation time based on the size of the spider silk proteins (250-350 kDa) would normally shorten the T_2 relaxation times considerably, destroying the resolution.
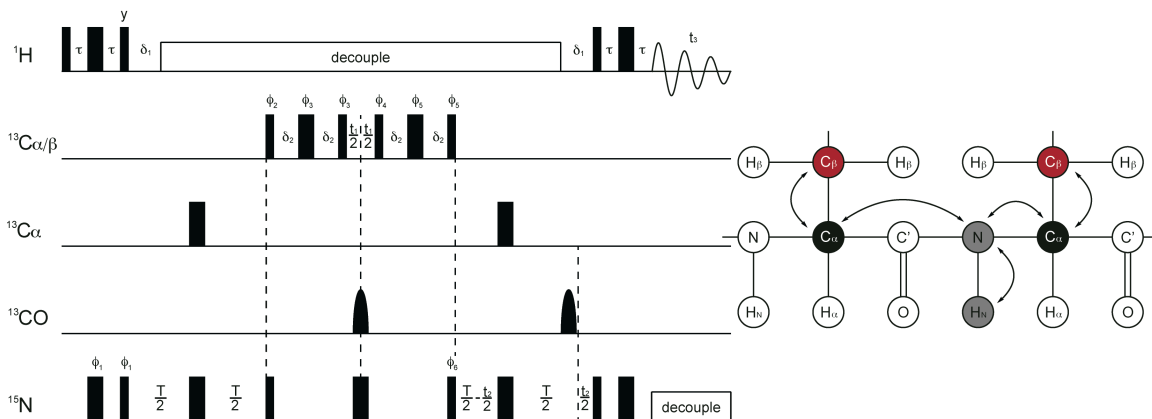

Fig. 12 The HNCACB triple resonance NMR pulse sequence for collecting 3D spectra. The polarization transfer mechanism is shown to the right. This sequence allows one to unambiguously assign ^{1}H/^{15}N HSQC spectra of isotopically enriched proteins. The NMR pulse sequence exploits the difference between ^{13}C–^{15}N J-couplings that are stronger for one bond (intra-residue) compared to two-bond (inter-residue) interactions.
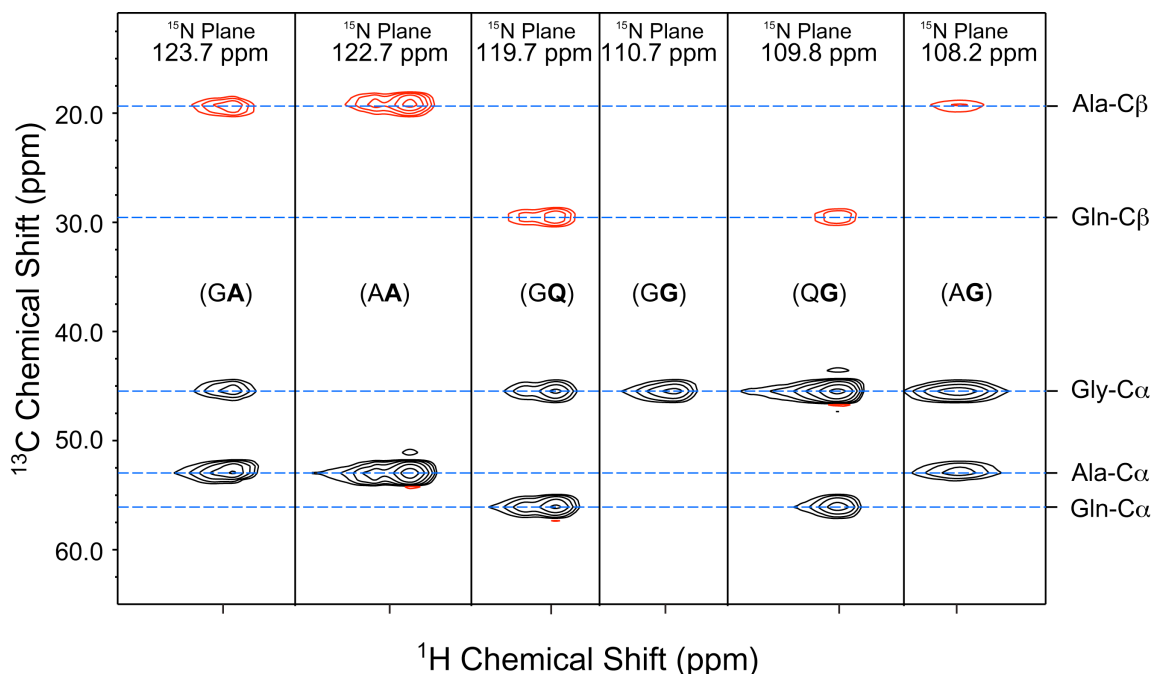
Fig. 13 The strip plots extracted from 3D HNCACB solution-state NMR experiment for U-[^{13}C/^{15}N]-alanine labeled major ampullate glands excised from the *Black widow* spider. The various ^{15}N planes are indicated in the figure along with the ^{13}C resonances that provide unambiguous resonance assignment. The negative contours are for the Cβ of the amino acid in primary amino acid sequence. The assignment of the NMR resonances is shown with one letter amino acid code. The bold letter is the amino acid group and the non-bolded letter is the previous amino acid to that amino acid in the primary sequence.

The reason that these conventional solution-state NMR experiments work has to do with the unfolded nature of the proteins with a high degree of local flexibility (see dynamic discussion below).

In order to assign the various resonances observed in the ^{15}N/^{1}H HSQC spectrum of *Black widow* major ampullate silk proteins (see Fig. 11) our research group has been exploring the utility of triple resonance (^{15}N/^{13}C/^{1}H) three-dimensional (3D) HR solution-state NMR pulse sequences on doubly labeled (^{13}C/^{15}N) silk protein samples. An example of one 3D NMR pulse sequence that we have been applying for resonance assignment of silk proteins is the HNCACB experiment (see Fig. 12). The HNCACB experiment allows one to unambiguously assign the protein backbone by correlating adjacent residues. The spectra are collected in the same way as a normal 2D ^{15}N/^{1}H HSQC with the addition of a third ^{13}C dimension. The pulse sequence takes advantage of differences between intra- and inter-residue ^{13}C-^{15}N through-bond J-couplings. The one bond J_{CN} coupling (intra-residue) is ~12 Hz while, the two-bond J_{CN} (inter-residue) is ~ 7 Hz. By taking advantage of the intensity differences between the various correlations one can distinguish intra- and inter-residue correlations and unambiguously assign the protein backbone.

Strip plots extracted from a recent 3D HNCACB triple resonance HR solution-state NMR experiment for doubly labeled Black widow major ampullate glands are shown in Fig. 13. The data is plotted such that the ^{1}H/^{13}C dimension is extracted for a given ^{15}N plane permitting backbone protein resonance assignment. For example, we can readily determine that the ^{15}N resonance at 123.7 ppm (left most strip plot) is an Ala
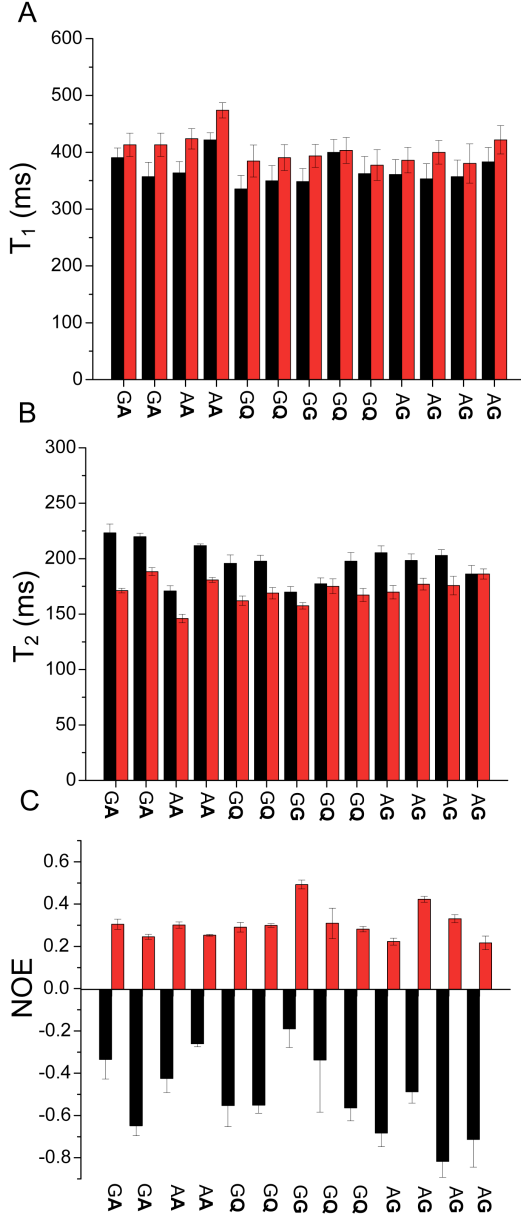
Fig. 14 The ^{15}N (A) T_1 relaxation, (B) T_2 relaxation and {^{1}H}/^{15}N heteronuclear NOE data measured with a ^{1}H/^{15}N HSQC pulse sequence for ^{15}N-alanine labeled *Black widow* major ampullate glands. The assignment of the NMR resonances is shown with one letter amino acid code. The bold letter is the amino acid group and the non-bolded letter is the previous amino acid to that amino acid in the primary sequence. All data was collected within 24 hrs of dissection to ensure that the silk proteins did not degrade or aggregate.

residue that is preceded by Gly in the primary amino acid sequence. This is determined by observing that the Ala-Cα is stronger than the Gly-Cα and the negative phase Ala-Cβ confirms that the preceding residue is Ala. Thus, this resonance represents Ala in a Gly-Ala group in the repetitive core of the spider silk protein. Utilizing this 3D NMR approach we have been able to establish a resonance assignment for all thirteen resonances observed in the ^{15}N/^{1}H HSQC spectrum of ^{15}N-alanine labeled *Black widow* major ampullate glands (see Fig. 11). Resonances can be assigned to Ala-Gly, Gln-Gly, Gly-Gly, and Ala-Ala residue pairs. An ability to unambiguously assign all the residues in the ^{15}N/^{1}H HSQC spectrum has now allowed us to study the backbone molecular dynamics of the silk proteins within the native gland environment with T_1/T_2 relaxation and heteronuclear NOE measurements.

The unstructured state of the spider silk proteins in the major ampullate gland points to the potential importance of the protein's dynamical features (*i.e.* flexibility) for the formation of silk fibers. We have begun interrogating the silk protein dynamics with ^{15}N T_1 and T_2 and {^{1}H}^{15}N heteronuclear NOE measurements. Based on the molecular weight of the spider silk proteins, conventional liquid-state NMR should be impossible or at minimum extraordinarily challenging requiring advanced HR solution-state NMR methods like transverse-relaxation optimized spectroscopy, TROSY (see M. Salzmann et al. *PNAS* **1998**, *95*, 13585). However, as can be seen in Fig. 11 and Fig. 13, conventional HR liquid-state protein NMR spectra are readily acquired on native, isotopically labeled silk proteins regardless of their large molecular weights (200 - 350 kDa). One can estimate the expected rotational correlation time of a globular protein from Stokes law:

$$\tau_c = 4\pi\eta \, r_H^3/(3k_BT)$$

(1)

where η is the viscosity of the solvent, r_H is the hydrodynamic radius of the protein, k_B is the Boltzmann constant and T is the temperature. The hydrodynamic radius can be estimated from the molecular weight of the protein in kDa, M_r:

$$r_H = [3\,\mathrm{V}M_r/(4\pi\mathrm{N}_A)]^{1/3} + r_w \qquad (2)$$

Fig. 15 The theoretical {¹H}¹⁵N NOE curves for (red) 800 and (black) 500 MHz as a function of correlation time (τ) in seconds. The average {¹H}¹⁵N NOE measured for [¹⁵N]-alanine labeled *Black Widow* major ampullate glands at the two field strengths is indicated with the blue dashed line.

where V is the specific volume of the protein, N_a is Avagadro's number and r_w is the radius of the hydration shell. If the silk proteins were folded globular proteins, we estimate a correlation time of 84 μs for a 300 kDa silk protein. This would render the solution-state NMR signals unobservable. The rotational correlation time must be in the nanosecond regime to yield well-resolved NMR resonances. The fact that we observe sharp NMR resonances indicates that the proteins must be unfolded and highly dynamic.

We have begun to probe the backbone dynamics of the silk proteins in the gland environment with ¹⁵N T_1 and T_2 relaxation and {¹H}¹⁵N NOE measurements. Results for these relaxation and NOE measurements on ¹⁵N-alanine labeled *Black widow* major ampullate glands are shown in Fig. 14 at two magnetic field strengths, 500 and 800 MHz. The relaxation times observed are quite long (T_1 = 325 - 400 ms and T_2 = 150 - 225 ms). Although there is some slight variability for the different residues, overall these long relaxation times are typically observed for globular proteins that are an order of magnitude smaller compared to the silk proteins. Even more striking are the observations for the {¹H}¹⁵N NOE measurements where large negative and small positive NOE's are observed at 500 MHz and 800 MHz, respectively. These observations are indicative of highly flexible groups that exhibit nanosecond dynamics.

In order to quantify the backbone dynamics further we have plotted the theoretical {¹H}¹⁵N NOE response (see Fig. 15) as a function of the correlation time (see L.E. Kay et al. *Biochemistry* **1989**, *28*, 8972 for theoretical background). The average NOE for the spider silk proteins in the major ampullate glands of *Black widow* spiders are presented along with the theoretical NOE at 500 and 800 MHz as function of correlation time (τ). The results of these NOE measurements indicate the presence of backbone dynamics of ~ 1 nanosecond confirming the highly flexible, unfolded state of the silk proteins in the major ampullate gland. In addition to probing the structure and dynamics of silk proteins within the major ampullate spider glands, we have been looking at the impact of various biochemical stimuli to further elucidate the conversion process from unstructured, isotropic silk dope to insoluble, structured high performance fiber. One biochemical parameter that we have been specifically focused on is pH. It is thought that during the silk producing process there is a lowering of pH from 7 to below 6 in the duct that initiates protein folding prior to spider silk fiber formation. To test this hypothesis, we
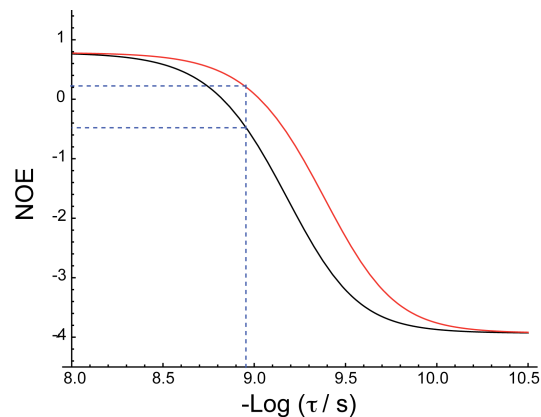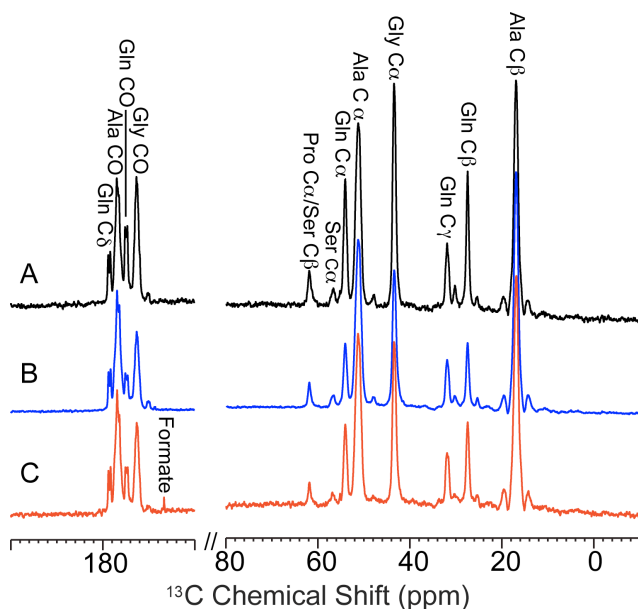
Fig. 16. The ^{13}C HR-MAS spectrum of *Black widow* major ampullate glands exposed to different acidification conditions, pH = (A) 6.0, (B) 3.1, and (C) 1.1. A probe molecule was added to the sample to measure pH. The formate pH probe is observed in (C). The silk proteins were isotopically enriched with U-[^{13}C/^{15}N]-alanine and the data was collected within 12 hrs of dissection.

have been studying the protein-rich gland fluid under various acidic conditions. Interestingly, we find little change in the ^{13}C HR-MAS NMR spectrum of the spider gland fluid under considerably acidic conditions (see Fig. 16). There is no chemical shift, line broadening or decrease in intensity observed for any of the ^{13}C resonances even at a pH as low as 1.1 within 12 hrs of exposing the glands to the acidic solvent. This result illustrates that there is not a spontaneous folding of the silk proteins upon lowering the pH and perhaps points to a combination of effects that initiate spider silk protein folding and fiber formation.

We have further explored the pH's for 24 hrs in a fridge at 4 °C. An example is shown in Fig. 17 where ^{13}C CP-MAS solid-state NMR spectra were collected for ^{13}C/^{15}N-alanine labeled *Black widow* major ampullate glands that were stored for 24 hrs at 4 °C. The ^{13}C solid-state NMR experiment with high power proton decoupling detects the formation of fibrous, protein β-sheet aggregates following the storage process for some samples. For a neutral pH of 7, there is no formation of β-sheet structures. In fact, in some cases, we have been able to store gland samples at neutral pH for months without β-sheet aggregates forming. At lower pH the results are quite different. At a pH of 6 a small amout of β-sheet structure forms however, at more acidic pH's of 2.7 and 1.8 considerable amounts of the protein are converted to fibrous, Ala-containing β-sheet structures following incubation at 4 °C for 24 hrs. It should be noted that these β-sheet structures are only observed when solid-state NMR is used. We are currently in the process of monitoring the kinetics of β-sheet formation as a function of pH with solid-state NMR.
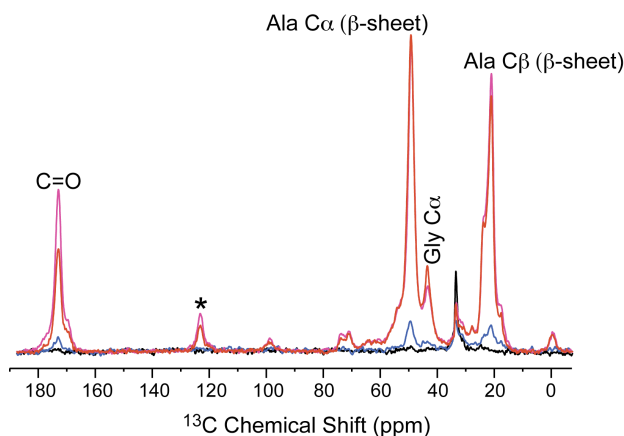

Fig. 17 The ^{13}C CP-MAS solid-state NMR spectrum of *Black widow* major ampullate glands exposed to different acidification conditions,and incubated at 4 °C for 24 hrs. pH = (black) 7.0, (blue) 6.0, (red) 2.7, (magneta) 1.8. The silk proteins were isotopically enriched with U-[^{13}C/^{15}N]-alanine.

In addition to NMR approaches to studying spider silk fiber formation, we have been developing XRD techniques in collaboration with Argonne National Laboratories at APS sector 11 and 14. XRD patterns for *Nephila clavipes* major and minor ampullate spider silks are shown in Fig. 18. These recently published results illustrate that the spider silk diffraction patterns can be deconvoluted into amorphous and nanocrystalline β-sheet fractions (S. Sampath et al. *Soft Matter*, **2012**, *8*, 6713). Using this approach the % crystallinity and crystallite size can be determined. We have been comparing the β-sheet crystalline fraction determined by XRD with those previously determined by our research group with solid-state NMR methods (J.E. Jenkins et al. *Biomacromolecules*, **2010**, *11*, 192). A comparison of the β-sheet fraction or %

Table 3. β-sheet fraction for spider silks from solid-state NMR and XRD

	Solid-state NMR	X-Ray
Major	34%	28%
Minor	45%	44%

crystallinity for *Nephila clavipes* major and minor ampullate spider silk determined by NMR and XRD is shown in Table 3. The results from the two techniques correlate well with good agreement observed within the error of the measurements (± 5%). It is readily determined from this combination of techniques that minor ampullate spider silk has a considerably higher β-sheet fraction compared to major ampullate spider silk. It should be noted that the original % crystallinity reported for *Nephila clavipes* major ampullate spider silk was 10 - 15% (Grubb et al. *Macromolecules* **1997**, *30*, 2860). Based on our combination of solid-state NMR and XRD methods it appears that this original % crystallinity is an underestimate.

The application of both solid-state NMR and XRD for characterizing spider silks will be powerful complimentary tools moving forward as XRD provides a true measure of crystallinity while, solid-state NMR identifies the residues that comprise the crystalline β-sheet nanostructures (*i.e*. Ala, Gly and Ser). In addition to determining the β-sheet fraction with X-ray techniques, our research team is also developing approaches with XRD to determine crystallite size, shape, and morphology. Recently, we developed an
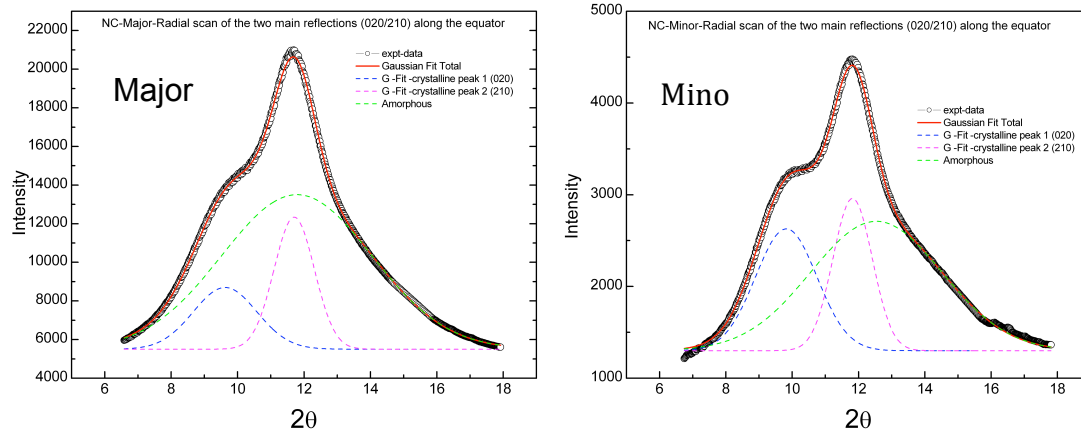

Fig. 18 The X-ray diffraction (XRD) patterns of (left) major ampullate and (right) minor ampullate spider silk collected from the Nephila clavipes species. The XRD patterns were deconvoluted into amorphous and crystalline components to extract the % crystallinity of the different spider silks. The results of the deconvolution are tabulated in Table 1.

approach to apply pair distribution function (PDF) measurements to obtain information regarding nanocrystallite size and shape. These results are highlight in a recently published *Phys. Rev. Lett.* manuscript titled "Total X-ray Scattering of Spider Dragline Silk" (C. Benmore et al. *Phys. Rev. Lett.* **2012**, 108, 178102).

In the past year, our research group has continued to develop MRI with localized spectroscopy as a tool to interrogate the silk producing glands *in situ* without sacrificing the spider and perturbing the gland environment by dissecting. Some recent results are presented in Fig. 19. The localized ^{1}H MRS spectrum and HR-MAS of the dissected major ampullate gland from the same Black widow spider following the MRI-MRS are strikingly similar. The silk protein resonances are nearly identical in the two spectra. There are some differences in the water region (4 - 5 ppm) of the spectrum that are due to better water suppression performance on the HR-MAS probe compared to the micro-imaging probe. However, the similarity between the protein resonances in the two ^{1}H NMR spectra illustrate that dissecting the spider and removing the major ampullate gland for HR-MAS and
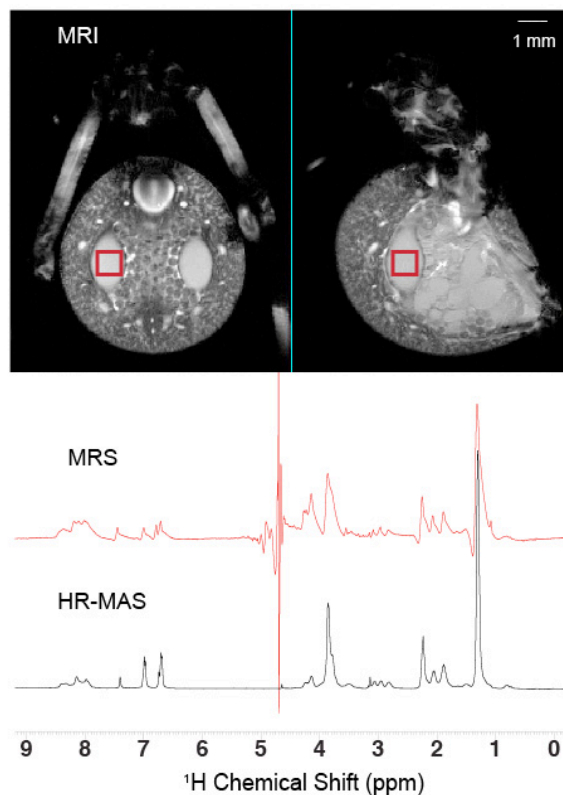

Fig. 19 Gradient echo ^{1}H T_2 weighted MRI of *Black widow* spider (top images) along with ^{1}H MRS and HR-MAS NMR spectrum of *Black widow* spider major ampullate glands. The red box on the MRI images indicates the localized voxel region where the ^{1}H MRS spectrum was spatially acquired. The ^{1}H HR-MAS NMR spectrum was acquired using the dissected major ampullate gland from the same spider in 90:10 H_2O:D_2O.

HR solution-state NMR measurements does not significantly perturb the silk protein structure.

4.3 Accomplishments/New Findings (Year 3):

In year 3 we continued to use a combination of solution- and solid-state NMR to characterize spider silk structure and dynamics in both the gland fluid and in solidified, insoluble silk fibers. A critical component of designing NMR experiments for structural and dynamic characterization of proteins in general, is determining the isotope (^{13}C/^{15}N/^{2}H) enrichment level for the different amino acid sites. It is also important to understand whether isotope scrambling occurs when attempting to isostopically label a single amino acid. In order to track isotope enrichment in spider silk proteins, we developed a method that utilizes ^{1}H solution-state NMR spectroscopy to determine the incorporation of isotopes on hydrolyzed spider silk fibers. To extract site-specific ^{13}C and ^{15}N isotope enrichments, an analysis method in Matlab was developed to fit the ^{1}H-^{13}C and ^{1}H-^{15}N J-splitting (J_{CH} and J_{NH}) ^{1}H NMR peak patterns of hydrolyzed silk fiber. This was demonstrated for *N. clavipes* spiders, where [U-^{13}C$_3$,^{15}N]-Ala and [1-^{13}C,^{15}N]-Gly
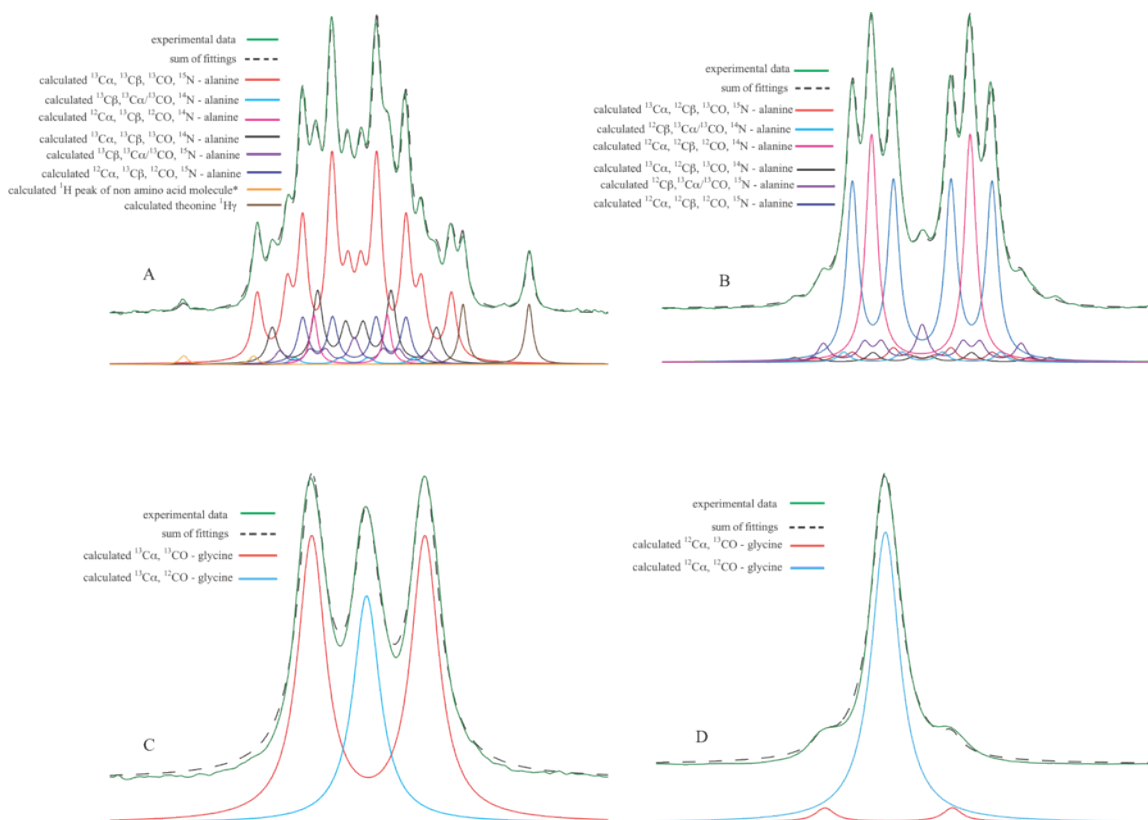
Fig. 20 Ala and Gly ^{1}H NMR peak fittings for [U-^{13}C$_3$,^{15}N]-Ala labeled *N. clavipes* dragline silk hydrolyzed in 6 M HCl for 3 days at 108 °C. The silk was collected on the 25th day during the isotope labeling process. (A) Fitting for Ala Hβ satellite transition peak of lower chemical shift. (B) Fitting for Ala Hβ central transition peak. (C) Fitting for Gly Hα satellite transition peak of lower chemical shift. (D) Fitting for Gly Hα central transition peak.

were separately dissolved in their water supplies and isotope incorporation was tracked over time (see X. Shi et al. *Anal. Bioanal. Chem.*, **2013**, *405*, 3997). An example of the ^{1}H NMR spectra that are obtained for hydrolyzed ^{13}C/^{15}N-isotopically enriched spider silks is shown in Fig. 20. The ^{1}H spectra are *J*-split due to the presence of ^{13}C/^{15}N-isotopes at different amino acid sites. This method can be used to extract the percent of each amino acid isotopomer for a given silk sample. We now use this methodology in our lab to track isotope incorporation in a site-specific way for different isotopic labeling schemes. The developed methodology can be applied to many fields, where site-specific tracking of isotopes is of interest.

Our research team recently developed a solution-state ^{1}H NMR method for determining the amino acid composition of hydrolyzed spider silk fibers. ^{1}H NMR spectroscopy experiments on acid hydrolyzed *N. clavipes* dragline silk was found to consist of 43.0±0.6% Gly, 29.3±0.2% Ala, 9.1±0.1% Glx, 4.0±0.1% Leu, 3.3±0.1% Tyr, 3.4 ±0.2% Ser, 2.7±0.1% Pro, 2.1±0.1% Arg, 1.07±0.05% Asx, 0.96±0.05% Val, 0.48±0.03% Thr, 0.35±0.03% Phe and 0.28±0.03% Ile. When compared with standard chromatography based Amino Acid Analysis (AAA), the chemical resolution of NMR allows for an amino acid solution to be characterized without separation and was shown to provide considerably higher precision (see X. Shi et al. *Anal. Biochem.*, **2013**, *440*,

150). This allows for more accurate statistics on the variability of amino acid contents in spider dragline silk. We were able to illustrate with this approach in spider dragline silk that Ala and Gly contents were conserved across samples (did not vary within error) while, Pro contents are highly heterogeneous (see Fig. 21). Because Pro is only located in the second spider silk protein, MaSp2, and not MaSp1, this result illustrates that the ratio of the two proteins varies considerably from sample to sample. In general, this ^{1}H NMR AAA technique is applicable to a large range of proteins and peptides for precise amino acid composition determination, especially when the precise content of a minor component is critical and relatively large amounts of sample are available (mg to mg quantities).
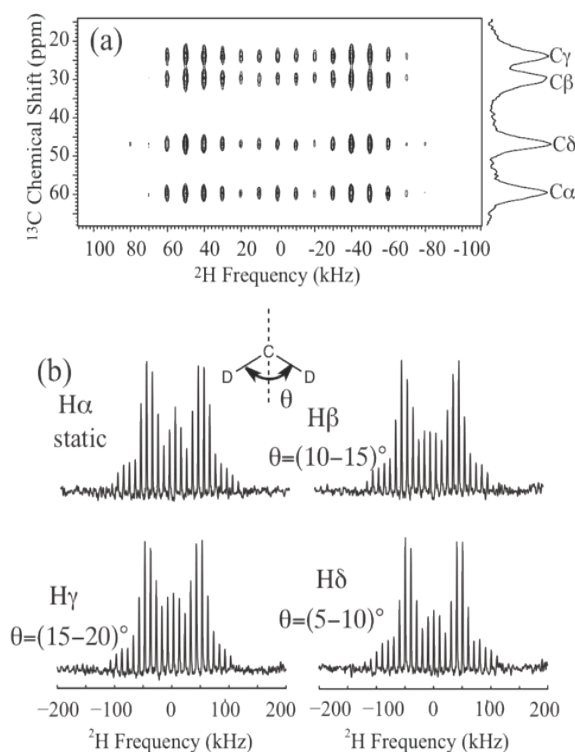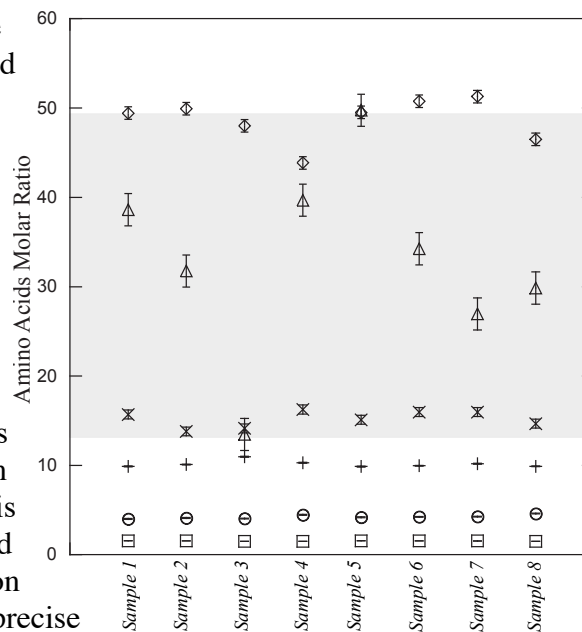
In addition to developing solution-state NMR spectroscopy to study spider silk proteins, we have been developing solid-state NMR techniques to interrogate

Fig. 21. Amino acid molar ratios for hydrolyzed *N. clavipes* dragline silk fibers determined by ^{1}H NMR. The displayed data are ratios for Gly/Ala (□), Gly/Glx (○), Gly/Leu (+), Gly/Tyr (✕), Gly/Pro (△) and Gly/Val (◇). The eight silk samples (~ 1 mg ea.) were produced from various spiders on the same diet. The grey box highlights the variability of the Gly/Pro ratios.

Fig. 22. The (a) 2D ^{2}H-^{13}C HETCOR MAS spectrum for U-[^{2}H$_7$,^{13}C$_5$,^{15}N]-Pro enriched *A. aurantia* dragline silk. (b) Pro ^{2}H line shapes extracted from the ^{13}C dimension and the proposed dynamics for each site. Pro side-chain dynamics is described as undergoing fast reorientation between two sites separated by an angle θ. The reorientation angles were obtained by comparing to simulated line shapes.

backbone and sidechain dynamics in spider silk fibers. We recently published a manuscript detailing an approach where ^{2}H→^{13}C cross polarization (CP) is used under MAS to indirectly-detect ^{2}H MAS powder patterns in a site specific manner with ^{2}H-^{13}C 2D HETCOR (see X. Shi et al. *J. Magn. Reson.* **2013**, *226*, 1-12). The extracted ^{2}H MAS powder patterns can then be simulated to extract information regarding the types of motions, timescales of motions and angles about which the motions occur. We have recently been applying this approach to understand the

backbone and sidechain dynamics in $^2H/^{13}C$-istopically enriched spider silk fibers. These experiments provide considerable information regarding the mobility (flexibility) of the backbone and sidechain groups in spider silks. These types of experiments should provide insight into the silk assembly process as the sidechain dynamics are influenced by the packing structure.

An example of ^2H-^{13}C 2D HETCOR MAS spectrum collected for U-[$^2H_7$,$^{13}C_5$,^{15}N]-Pro labelled *A. aurantia* dragline silk is shown in Fig. 22. The Pro side-chain molecular motions are best described by each deuterium undergoing a two-site reorientation about a given angle. To interpret this motion for each site, ^2H line shape simulations were conducted and compared with the experimental data. The simulations illustrated that each deuterium on the side-chain undergoes fast two sites reorientation at an angle of $(15-10)°$, $(15-20)°$ and $(5-10)°$ for Pro $^2H\beta$, $^2H\gamma$ and $^2H\delta$, respectively (see Fig. 22b). The corresponding reorientation motion rates are larger than 10^8 s^{-1}. Interestingly, the Pro residues in spider dragline silk (the MaSp2, GPGXX motif) undergo smaller reorientation angles, when compared to a standard crystalline proline sample indicating that the Pro sidechain has a lower degree of flexibility in spider silk

Fig. 23 The (a) ^2H solid-echo spectra for U-[$^2H_7$,$^{13}C_5$,^{15}N]-Pro labelled *A. aurantia* dragline silk in the dry and wet, supercontracted state. (b) ^2H solid echo spectrum of supercontracted silk (blue, same as show in (a) and its fit (green). The center peak region is expanded and shown on the upper right. Two components (red and black) are extracted from the fit. The asterisks indicate the spinning sidebands. (c) Comparison of experimental (black) and simulated ^2H line shape (red). The experimental line shape is the broad component extracted from the fit data (shown in black in (b). Spectra simulated with three sites reorientation along an external axis with a rate of $3×10^6$ s^{-1} (the schematic representation of the motion is shown in the upper right).

compared to the proline crystal. This is somewhat surprising since, the Pro containing motif is often touted as the flexible region in spider silk. However, the dynamic results from these experiments indicate that the flexibility in spider silk is lower compared to crystalline proline.

The Pro-containing GPGXX motif in spider silk is believed to be responsible for the silk's supercontraction phenomenon. We have been exploiting ^2H MAS NMR methods to interrogate the dynamics for the Pro when the silk is supercontracted in water. Our initial attempts to utilize the ^2H-^{13}C HETCOR MAS approach described above were ineffective. For the wet, supercontracted silk, the ^2H-^{13}C CP signal was undetectable with reasonable NMR experimental collection times. This indicates that the Pro-containing motifs interact strongly with intercalated water and become highly dynamic when the silk
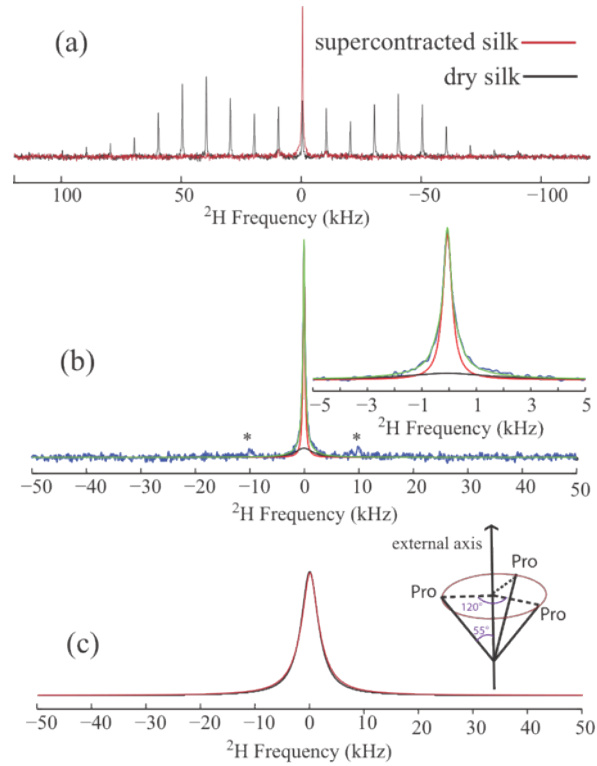
is supercontracted. The large Pro ^{2}H MAS powder pattern observed in the dry silk is reduced to a central peak accompanied by weak spinning sidebands (see Fig. 23). Additionally, a significant signal loss (30-35%) was observed for the wet, supercontracted silk in a fully relaxed ^{2}H one pulse and solid-echo NMR experiments (see Fig. 23a,b). The center peak cannot be fit by a single resonance possessing a Lorentzian, Gaussian or combination lineshape. Instead, fits of ^{2}H 1D data indicate the existence of two components, one narrow and one broad. ^{2}H signal loss is due to the short T_2 of the broad component, a consequence of molecular motion in the 10^6 s^{-1} regime according to our initial simulations. We are currently in the process of utilizing ^{2}H simulations to describe the backbone and sidechain motions for Pro in wet, supercontracted silk. However, the considerable change in the ^{2}H MAS powder pattern when the silk is water-wetted (supercontracted) indicates that the molecular dynamics of the spider silk protein GPGXX region is enhanced considerably.

Finally, in addition to developing NMR and XRD techniques to characterize the structure and dynamics of spider silk proteins, our research team has been exploring the utility of Brillouin spectroscopy for probing the mechanical properties of processed spider silk glands (see Koski et al. Appl. Phys. Lett. 2012, 101, 103701) and intact spider webs (see Koski et al. Appl. Phys. Lett. 2012, 101, 103701). This method is a laser-based non-invasive, non-destructive method for characterizing the silk proteins in sheared silk glands and when spun into spider silk webs. These Brillouin spectroscopic measurements completely quantify the linear elastic response for all possible deformation modes, information unobtainable with traditional stress–strain tests.

5. Personnel Supported:
Gregory P. Holland (PI), Supported three months of summer salary
Jeffery L. Yarger (co-PI), Supported six weeks of summer salary
Xiangyan Shi (Ph.D. Student, Research Assistant), Supported 25 months.
Dian Xu (Ph.D. Student, Research Assistant), Supported 5 months.
Chengchen Guo (Ph.D. Student, Research Assistant), Supported 2 weeks.
Joel Ayon (Undergraduate Student, Part-time Researcher), Supported 150+ hrs.
Brandon Blass (Undergraduate Student, Part-time Researcher), Supported 500+ hrs.
Barbara Brenneman (Undergraduate Student, Part-time Researcher), Supported 160+ hrs.

6. Publications:
1) Jenkins, J.E., Sampath, S., Butler, E., Kim, J., Henning, R.W., Holland, G.P., Yarger, J.L. "Characterizing the Secondary Protein Structure of Black Widow Dragline Silk Using Solid-state NMR and X-ray Diffraction" *Biomacromolecules* **2013**, *Accepted*.

2) Holland, G.P., Mou, Q., Yarger, J.L. "Determining Hydrogen-bond Interactions in Spider Silk with ^{1}H-^{13}C HETCOR Fast MAS Solid-state NMR and DFT Proton Chemical Shift Calculations" *Chem. Commun.* **2013**, *49*, 6680-6682.

3) Shi, X., Yarger, J.L., Holland, G.P. "Probing Site-specific ^{13}C/^{15}N-isotope Enrichment of Spider Silk with Liquid-state NMR Spectroscopy" *Anal. Bioanal. Chem.* **2013**, *405*, 3997-4008.

4) Shi, X., Holland, G.P., Yarger, J.L. "Amino Acid Analysis of Spider Dragline Silk Using ^{1}H NMR Spectroscopy" *Anal. Biochem.* **2013**, *440*, 150-157.

5) Addison, J.B., Ashton, N.N., Weber, W.S., Stewart, R.J., Holland, G.P., Yarger, J.L. "β-sheet Nanocrystalline Domains Formed from Phosphorylated Serine-rich Motifs in Caddisfly Larval Silk: A Solid-state NMR and XRD Study" *Biomacromolecules* **2013**, *14*, 1140-1148.

6) Koski, K.J., Akhenblit, P., McKiernan, K., Yarger, J.L. "Non-invasive Determination of the Complete Elastic Moduli of Spider Silks" *Nature Materials* **2013**, *12*, 262-267.

7) Asakura, T., Suzuki, Y., Nakazawa, Y., Yazawa, K., Yarger, J.L., Holland, G.P. "Silk Structure Studied with Nuclear Magnetic Resonance" *Prog. Nucl. Mag. Res. Sp.* **2013**, *69*, 23-68.

8) Shi, X., Yarger, J.L., Holland, G.P. "^{2}H-^{13}C HETCOR MAS NMR for Indirect Detection of ^{2}H Quadrupole Patterns and Spin-lattice Relaxation Rates" *J. Magn. Reson.* **2013**, *226*, 1-12.

9) Gnesa, E., Yang, H., Yarger, J.L., Warner, W., Lin-Cereghino, J., Lin-Cereghino, G., Tang, S., Agari, K., Vierra, C. "Conserved C-Terminal Domain of Spider Tubuliform Spidroin 1 Contributes to Extensibility in Synthetic Fibers" *Biomacromolecules* **2012**, *13*, 304-312.

10) An, B., Jenkins, J.E., Sampath, S., Holland, G.P., Hinman, M., Yarger, J.L., Lewis, R.V. "Reproducing Natural Spider Silk's Copolymer Behavior in Synthetic Silk Mimics" *Biomacromolecules* **2012**, *13*, 3938-3948.

11) Benmore, C., Izdebski, T., Yarger, J.L. "Total X-ray Scattering of Spider Dragline Silk" *Phys. Rev. Lett.* **2012**, *108*, 178102.

12) Sampath, S., Izdebski, T., Jenkins, J.E., Ayon, J.V., Henning, R.W., Ogel, J.P.R.O., Antipoa, O., Yarger, J.L. "X-ray Diffraction Study of Nanocrystalline and Amorphous Structure within Major and Minor Ampullate Dragline Spider Silks" *Soft Matter* **2012**, *8*, 6713-6722.

13) Koski, K.J., McKiernan, K., Akhenblit, P., Yarger, J.L. "Shear Induced Rigidity in Spider Silk Glands" *Appl. Phys. Lett.* **2012**, *101*, 103701.

14) Blanchard, J.W., Groy, T.L., Yarger, J.L., Holland, G.P. "Investigating Hydrogen-bonded Phosphonic Acids with Proton Ultrafast MAS NMR and DFT Calculations" *J. Phys. Chem. C.* **2012**, *116*, 18824-18830.

15) Jenkins, J.E., Holland, G. P., Yarger, J. L. "High Resolution Magic Angle Spinning NMR Investigation of Silk Protein Structure within Major Ampullate Glands of Orb Weaving Spiders" *Soft Matter* **2012**, *8*, 1947-1954.

16) Teule, F., Addison, B., Copper, A.R., Ayon, J., Henning, R.W., Benmore, C.J., Holland, G. P., Yarger, J. L., Lewis, R. V. "Combining Flagelliform and Dragline Spider Silk Motifs to Produce Tunable Synthetic Biopolymer Fibers" *Biopolymers* **2012**, *97*, 418-431.

17) B. An, M.B. Hinman, G.P. Holland, J.L. Yarger, and R.V. Lewis "Inducing β-sheets Formation in Synthetic Spider Silk Fibers by Aqueous Post-spin Stretching," *Biomacromolecules*, **2011**, *12*, 2375-2381.

18) J.W. Blanchard, J.-P. Belieres, T.M. Alam, J.L. Yarger, and G.P. Holland "NMR Determination of the Diffusion Mechanisms in Triethylamine-based Protic Ionic Liquids," *J. Phys. Chem. Lett.*, **2011**, *2*, 1077-1081.

19) M.S. Creager, J.E. Jenkins, L.A. Thagard-Yeaman, A.E. Brooks, J.A. Jones, R.V. Lewis, G.P. Holland, J.L. Yarger "Solid-state NMR Comparison of Various Spiders' Dragline Silk Fiber," *Biomacromolecules*, **2010**, *11*, 2039-2043.

20) J.E. Jenkins, M.S. Creager, E.B. Butler, R.V. Lewis, J.L. Yarger, G.P. Holland "Solid-state NMR Evidence for Elastin-like β-Turn Structure in Spider Dragline Silk," *Chem. Commun.*, **2010**, *46*, 6714-6716.

7. Interactions/Transitions:

a. Participation/presentations at Meetings, Conferences, Seminars:
1) Gregory P. Holland, "Combining Solid-state and HR-MAS NMR Methods to Investigate Conformational Structure and Mobility of Spider Silk Proteins" Rocky Mountain Conference on Analytical Chemistry, July 2010.

2) Gregory P. Holland, "Elucidating Structure and Dynamics in Spider Silk with Multi-dimensional Multinuclear Solid-state MAS NMR" Pacifichem, December 2010.

3) Gregory P. Holland, "Spider Gland Fluids: From Protein-rich Isotropic Liquid to Insoluble Super fiber" DOD-AFOSR, 2312 EX and DX (Natural Materials, Systems and Extremophiles) Program Review, January (2011).

4) Jeffery L. Yarger, "Diffraction and Scattering of Silk Fibers" Oak Ridge National Labs, Spallation Neutron Source Division, October (2010).

5) Jeffery L. Yarger, "Biopolymers Stretched to the Limit" Dynamic Phenomena Under Extremes, UT Austin, January (2011).

6) Jeffery L. Yarger, "NMR of Silk and Related Biopolymers" University of Michigan, Department of Chemistry, October (2010).

7) Jeffery L. Yarger "Structure and Dynamics of Natural and Synthetic Spider Silk Proteins" University of Utah, Department of Physics, February (2011).

8) Holland, G.P., "Structural Characterization of Spider Silk and the Silk Producing Process with Magnetic Resonance Methods" NYC Silk Workshop, Silk: Is it All Spin?, NY Academy of Sciences, NY, NY, July (2011).

9) Yarger, J.L. "Magnetic Resonance of Spiders and Silk" American Arachnological Society Meeting, Portland, OR, July (2011).

10) Yarger, J.L. "XRD of Spider Silk Fibers" Argonne National Laboratory User Meeting, Argonne, IL, October (2011).

11) Yarger, J.L. "Spider Silk – Nature's Amazing and Diverse Copolymer" Biology Colloquium, Santa Clara University, Santa Clara, CA, August (2011).

12) Yarger, J.L. "Neutron Scattering of Glasses and Biopolymers" Oak Ridge National Laboratory, Neutron and X-ray Scattering Workshop, Oak Ridge, TN, Sept (2011).

13) Holland, G.P. and Yarger, J.L. "Spider Gland Fluids: From Protein-rich Isotropic Liquid to Insoluble Super fiber" DOD-AFOSR, 2312 EX and DX (Natural Materials, Systems and Extremophiles) Program Review, National Harbor, MD, December (2011).

14) Yarger, J.L. "Basics of Solid-State NMR for Materials Characterization" RUSTEC Workshop, Principles and Practice of Nanomaterials Characterization, Arizona State University, Tempe, AZ, December (2011).

15) Holland, G.P., "Structural Characterization of Spider Silk with NMR Methods" American Chemical Society 243th National Meeting, San Diego, CA, March (2012).

16) Cherry, B.R., Holland, G.P., Xu, D., Yarger, J.L., "MRI of Black Widow Spiders" Experimental NMR Conference, Miami, FL, April (2012).

17) Shi, X., Holland, G.P., Yarger, J.L., "Characterization of Structure and Dynamics in Spider Silk with ^{2}H-^{13}C Correlation NMR Experiments" Experimental NMR Conference, Miami, FL, April (2012).

18) Holland, G.P., "Exploring Structure - Function Relationships in Spider Silk with NMR" Departmental Seminar - Chemistry, Physics and Biology, Brooklyn College, NY, NY, June (2012).

19) Holland, G. P., "Exploring Structure-Function Relationships in Spider Silk with Magnetic Resonance" Talloires Silk Workshop, Silk: Threads of New Discovery" Talloires, France, July (2012).

20) Holland, G.P., "Spider Gland Fluids: From Protein-rich Isotropic Liquid to Insoluble Super fiber" DOD-AFOSR, 2312 EX and DX (Natural Materials, Systems and Extremophiles) Program Review, Washington DC, January (2013).

21) Yarger, J.L., "Molecular Level Elucidation of Biopolymers" University of Arizona, Materials Science Department, Tucson, AZ, March (2013).

22) Yarger, J.L., "Understanding Complex Macromolecular and Supramolecular Systems using Innovative Magnetic Resonance Strategies" American Chemical Society 245th National Meeting, New Orleans, LA, April (2013).

b. Consultive and Advisory Functions: None
c. Technology Assists, Transitions, and Transfers: None

8. New discoveries, inventions, or patent disclosures: None

9. Honors/Awards: None